Soft Matter

Accepted Manuscript

ROYAL SOCIETY OF CHEMISTRY

www.rsc.org/softmatter

Unique effect of the electric field on a new liquid crystalline lactic acid derivative

Vladimíra Novotná,[a] Milada Glogarová,[a] Miroslav Kašpar,[a] Věra Hamplová,[a] Lubor Lejček,[a] and Damian Pociecha[b]

[a] *Institute of Physics, The Czech Academy of Sciences, Na Slovance 2, CZ-182 21 Prague 8, Czech Republic*
[b] *Laboratory of Dielectrics and Magnetics, Chemistry Department, Warsaw University, Al. Zwirki i Wigury 101, 02-089 Warsaw, Poland*

Abstract
A new chiral lactic acid derivative is presented, exhibiting a frustrated liquid crystalline phase, namely the orthogonal twist grain boundary TGBA phase in a broad temperature interval. Unique effect is observed and found that the applied electric field reversibly transforms the planar TGBA texture to the homeotropic one, homogeneously dark in crossed polarizers. The transformation is an analogy of the Frederiks transition known in nematics, in which the switching under the field is driven by the positive dielectric anisotropy. Similar effect is established also in the SmA phase of the racemic mixture, where the transformation under the field is irreversible. Positive dielectric anisotropy in both chiral compound and racemic mixture is detected up to the field frequency of about 10 kHz, above this frequency the anisotropy is negative. The unusual behavior of the TGBA phase under the electric field can be explained by the specific packing of molecules within the smectic layers, resulting in relatively high layer compressibility, which lowers the energy of structural defects and thus facilitates the structure transformation. The perfectly dark state of studied compounds, induced by the electric field, either stable or reversible, is appealing for specific applications. The change of the sign of the dielectric anisotropy, known in nematics as the dual frequency effect, might be important for photonics such as adaptive or diffractive optics.

Introduction

Liquid crystals (LCs) are highly fluid self-assembling media revealing the complexity of physical properties as well as providing a powerful tool for multidisciplinary research. From the application aspect, the reorientation of nematics under the applied electric field is a fundamental phenomenon, which is widely used in modern technologies. Self-assembling properties of LCs are strictly linked to the shape and chemical structure of the molecules.[1] A variety of forces influences the packing of molecules and results in a wide number of liquid crystalline phases. In addition, for chiral molecules a tendency to form helical structures appears. Interactions promoting self-assembling of molecules into layers are very important and a strong competition between tendencies to layering and twisting might lead to the existence of frustrated structures such as Blue Phases (BPs),[2] Twist Grain Boundary (TGB),[3] and the SmQ phases.[4] The structures of these phases are inevitably accompanied with defects, which has a significant impact on their forming, textures and properties.

The existence of TGB phases was first predicted by de Gennes[5] and theoretically described by Renn et all.[6] Afterwards, the TGB phase was discovered by Goodby.[7] The TGB phase can be regarded as a liquid crystalline analog of Abrikosov vortex superconductors and the cholesteric (N*) – smectic A (SmA) phase transition is similar to a normal metal – superconductor transition in a magnetic field.[8] In the liquid crystalline phase the director, describing the average orientation of the long molecular axis, is analogous to the magnetic vector potential and the chirality plays a role of the magnetic field. In the TGB phase small blocks of a smectic phase are rotated with respect to each other, being separated by systems of screw dislocations forming *twist boundary*. A helical axis is parallel to the plane of smectic layers with the pitch typically in the range of the visible light wavelength.

So far several types of TGB phases have been identified and described.[9] The most common are the TGBA phase, composed of the blocks (slabs) of the orthogonal SmA, and the TGBC phase with the blocks of a tilted SmC phase. We will concentrate on the first one, the TGBA phase, which is paraelectric and mostly observed only in a narrow temperature interval below the BP or the N* phase, but may also appear directly below the isotropic phase. Exceptionally, the TGBA phase appears as a re-entrant phase below the SmA phase.[10]

Generally, the textures of the TGB phases observed in the polarized light of the optical microscope are diverse and complicated, exhibiting various features depending on the sample thickness, surface, geometries.[11] Two types of sample geometry exist depending on the anchoring of molecules at the sample surface. Under the *planar* anchoring the long axes of molecules (director) become parallel to the sample plane, while the *homeotropic* anchoring promotes the perpendicular orientation of molecular director to the sample plane. The homeotropic anchoring is also realized in *free standing films*, in which the melted substance is spread out over a circular hole (diameter 2 mm) in an aluminium or glass plate.

Due to the inevitable presence of defects in the TGB phases, typical features of textures of these phases survive in the subsequent non-frustrated phase on heating or on cooling (paramorphic features). Thus, the paramorphic features make texture characterization more difficult and the thermal history of the sample is important. In free standing films as well as in samples with the homeotropic anchoring the filament or fingerprint textures typically occur,[12,13] sometimes a low-birefringent texture similar to the fan-shaped textures in classical smectic phases may be formed.[10c,13] Under the planar anchoring mostly a blurred fan-shaped texture occurs, less frequently oily-streak or irregular-grain textures appear with variable colors corresponding to the pitch length of the TGBA block rotation.[12]

Until the TGB phase discovery the helical structure had been observed only in several liquid crystalline phases created of rod-like mesogens, namely nematics and tilted smectics. In the TGBA phase a strong chirality enforces the helix even if the structure in blocks shows no twist. The TGBA phase reveals the following basic features: layered structure and a helical superstructure with the helical axis perpendicular to the director. Generally, an external filed can expel the defects from the structure and the TGBA phase can be turned to the regular SmA phase. Additionally, under an electric field the electroclinic effect can be observed in analogy to the SmA phase of chiral compounds.[14]

Herein we report the study of a new chiral rod-like compound revealing the TGBA phase and unusual effects under the applied electric field are explored. For better understanding of this phenomenon and stability of the TGBA phase, we prepared the racemate and compared the effect of the electric field.

Experimental

Synthesis of studied compounds

The chemical structure of the studied compound *(S)-1-oxo-1-(pentyloxy)propan-2-yl 4-((4-(dodecyloxy)benzoyl)oxy)benzoate* denoted PHB(S) is depicted in Scheme 1 with the synthetic route of its preparation. Details concerning synthesis of the intermediates are presented in ESI. *N,N´*-dicyclohexylcarbodiimide (3.1 g,15 mmol) was added with stirring to a solution of 2.8 g (10 mmol) of phenol 2 (Scheme 1), 3.1 g (10 mmol) of 4-(dodecyloxy)benzoic acid and 1 mmol of 4-pyrrolidinopyridine in 100 ml of CH_2Cl_2. After stirring for 12 hours at a room temperature the precipitate (*N,N´*-dicyclohexylurea) was removed, the filtrate was evaporated and crude product chromatographed on silica gel (Kieselgel 60, Merck Darmstadt) using CH_2Cl_2 as an eluent. Pure compound (more than 99.8 % according normal phase HPLC with 99.9 % of toluene and 0.1 % of methanol as a mobile phase) was obtained after crystallization from methanol in yield 5.32 g (94 %). Specific rotation was found $[\alpha]_D^{25} = +9.0°$ (c= 0.2, $CHCl_3$).

^{1}H- NMR of PHB ($CDCl_3$):

0.9 (6H, m, $\underline{CH_3}CH_2$), 1.20 -1.56 (18H, m, CH_2), 1.56 -1.72 (5 H, d, $\underline{CH_3}C^*H$, 1.68, J=7.1 Hz and $COOCH_2\underline{CH_2}$), 1.84 (2H, quint., J=7 Hz, $ArOCH_2\underline{CH_2}$), 4.06 (2H, t, J= 6.5 Hz, Ar-OCH_2), 4.18 (2H, dt, J_1=6.5 Hz, J_2= 2.1 Hz, $COOCH_2$), 5.35 (1H, q, J=7.1 Hz, C*H), 7.00 (2H, d, J=9 Hz, H-Ar *ortho* to OR), 7.34 (2H, d, J=8.7 Hz, H-Ar *meta* to COO-CH*), 8.18 (4H, 2d, J=8.5 Hz, H-Ar *meta* to OR and *ortho* to –COOC*H).

Analogous procedure was used for the preparation of racemic material PHB(rac) using racemic *n*-pentyl lactate as a starting material.

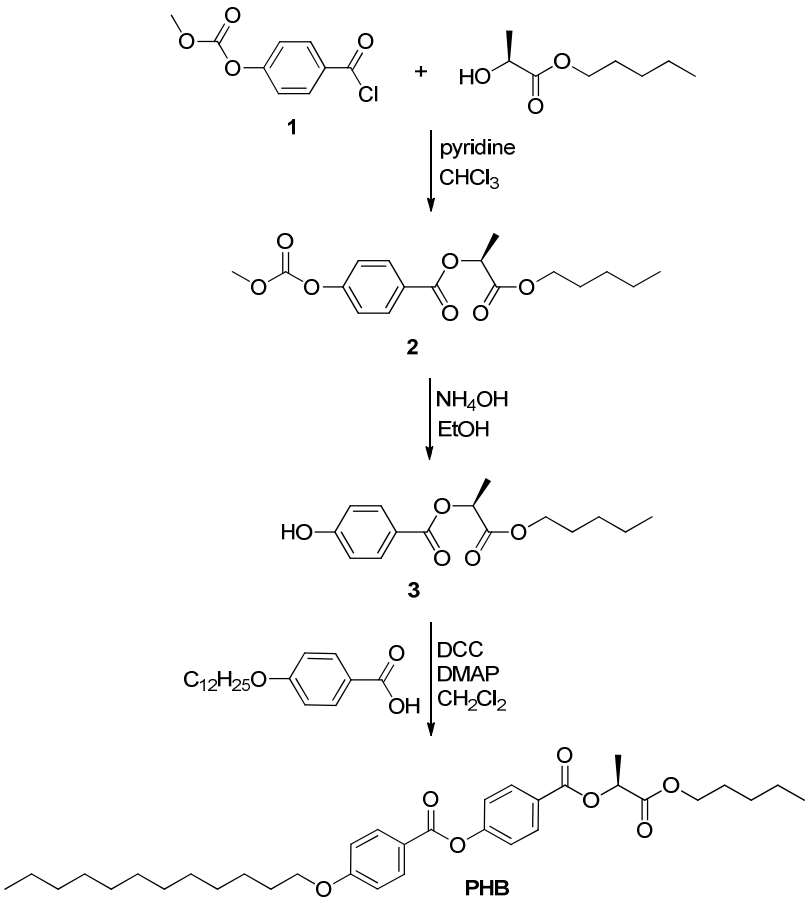

Scheme 1
Synthetic route for the preparation of studied compound PHB.

Set-up and measurements

Differential scanning calorimetry (DSC) measurements were performed using Pyris Diamond Perkin-Elmer 7 apparatus. The phase transition temperatures and enthalpies were determined on cooling and heating runs at a rate of 5 K/min. The samples of 2-5 mg weight were hermetically closed in aluminium pans and placed into the calorimeter chamber. The cells for texture observation and electro-optical studies were prepared from the glass plates covered by ITO transparent electrodes (5x5 mm^2). The planar anchoring is ensured using a surfactant and with rubbing along the electrode edge (easy direction). In such a sample the molecules are anchored at the surface with the molecular long axis parallel to the easy direction. Commercial cells were purchased from AWAT comp., Warsaw. Cells were filled by capillarity action in the isotropic phase. Texture observations were performed using Nikon Eclipse polarizing microscope, equipped with a Linkam hot stage. For texture studies also cells composed of glasses without any surface treatment were used. In the contact probe sample the compounds are soaked by capillary action in the opposite sides of the cell at the same time.

Frequency dispersion of permittivity was measured on cooling using Schlumberger 1260 impedance analyser in a frequency range of 1 Hz ÷ 1 MHz, keeping the temperature of the

sample stable within ±0.1 K during the frequency sweeps. The frequency dispersion data were analysed using the Cole-Cole formula for the frequency dependent complex permittivity, complemented by the second and the third terms to eliminate the low frequency contribution from d.c. conductivity, σ, and the high frequency contribution due to the resistance of the ITO electrodes, respectively:

$$\varepsilon^* - \varepsilon_\infty = \frac{\Delta\varepsilon}{1 + (if / f_r)^{(1-\alpha)}} - i\left(\frac{\sigma}{2\pi\varepsilon_0 f^n} + Af^m\right) \quad (1),$$

where f_r is the relaxation frequency, $\Delta\varepsilon$ is the dielectric strength, α is the distribution parameter of relaxation, ε_0 is the permittivity of vacuum, ε_∞ is the high frequency permittivity and n, m, A are the parameters of fitting. Measured real, ε', and imaginary, ε'', parts of permittivity $\varepsilon^*(f) = \varepsilon' - i\varepsilon''$ were simultaneously fitted to formula (1).

The smectic layer thickness, d, was determined from the small angle x-ray diffraction studies, according to Bragg's law, $n\lambda = 2d\sin\theta$, were θ is the diffraction angle. The measurements were performed with Bruker D8 Discover diffractometer (Cu Kα radiation, λ = 1.54 Å, Goebel mirror monochromator, scintillation counter), equipped with a heating stage (Anton Paar DCS350), assuring temperature stability within ±0.1 K. Samples were prepared as thin films on a heated silicon wafer. Diffraction experiments in broad angle range were done using Bruker GADDS system (Cu Kα radiation, Goebel mirror monochromator, point collimator, area detector Vantec 2000).

Results

We have characterized the mesomorphic properties of both studied compounds, chiral PHB(S) and its racemic mixture PHB(rac). We performed DSC measurements and concluded that for chiral PHB(S) one mesophase exists on heating within the temperature range from 25°C to 33°C (see Fig. 1a). On cooling the temperature range of the mesophase occurrence is much broader due to supercooling effect. Based on texture observation and structural studies we identified the observed mesophase for PHB(S) as the TGBA phase (we will explain in details later). On cooling runs DSC signal at the transition from the isotropic phase to mesophase is split into two peaks (the inset in Fig. 1), the low temperature one corresponding to the transition, the additional broad signal can be related to strong pre-transitional effect, which is often observed for the TGBA phase on cooling. For a direct phase transition from the isotropic phase to the TGBA phase this effect on the DSC thermograph has been found and described by Goodby et al.[7a] for the first time. It has been supposed that above the transition to the TGBA phase an intermediary liquid phase exists with short range SmA ordering of the molecules in clusters surrounded by a liquid.[7] The DSC plot for the PHB(rac), shown in Fig. 1b, exhibits no mesophase on heating, but on cooling a monotropic mesophase appears at 34°C that can be strongly overcooled. No crystallization occurs on cooling down to -20°C, it takes place on subsequent heating run (Fig. 1b). The peak corresponding to the isotropic-SmA phase transition on cooling is very sharp and the existence of another narrow mesophase above the TGBA phase can be excluded. The optical

purity affects the mesophases stability and the phase transition temperatures. Usually in liquid crystalline compounds the racemate has higher clearing temperature, which has been observed also for PHB compound. We prepared and studied a binary mixture 50:50 of PHB(S) and PHB(rac) denoted as Mix 1:1. We have found that such mixture exhibits a lower melting point than pure PHB(rac). One can conclude that our racemate is a true racemate, not a racemic conglomerate. The enthalpy values, ΔH, melting points, m.p., phase transition temperatures, T_r, obtained from the DSC data for both studied materials and the binary mixture are presented in Table 1.

In the planar sample of the chiral compound PHB(S) a typical planar texture of the TGBA phase is observed in crossed polarizers on cooling down below the isotropic phase, see Fig. 2. This texture contains colored grains, with the color corresponding to the pitch length of the TGB helix and with the helical axis perpendicular to the sample plane. Changes of the color with the temperature are clearly seen on the planar sample in a temperature gradient (Fig. 3). Based on the observations, we can estimate the value of the pitch length changing from 380 to 750 nm on decreasing temperature within the temperature interval 32.9°C to 31.8°C. For lower temperatures the pith value is probably higher than the wavelength of the visible light and we are not able to evaluate it more precisely. We can extrapolate and expect the pitch value to be 2-3 μm at temperatures about 26°C, which is a reasonable value for the TGBA phase.

Rather surprising behavior of textures has been observed in an electric field. The electric field changes the planar texture of the TGBA phase into a homogeneously dark state, showing optically uniaxial symmetry with the optical axis perpendicular to the sample surface, which evidences a perfectly aligned SmA phase with layers parallel to glass substrates. Behavior of the sample after switching off the field depends on temperature - in the temperature interval 33°C down to 28°C the filaments grow in the homogeneously dark structure, while in temperatures below 27 °C the homeotropic texture is stable. Changes of the optical texture in a planar 5 μm thick cell are shown in Fig. 4. The upper part of the photograph area is outside the electrode and show the virgin texture in comparison with the lower part, which was turned into homogeneously dark by the electric field of 10 V/μm. In Figs. 4b and 4c the gradual nucleation of filaments is presented 2 and 4 seconds after the electric field is switched off, respectively. Apparently the orientation of filaments is not random, but they make a certain angle between 45 and 50 degrees with respect to the easy direction. Thus two systems of parallel filaments are created, which are nearly perpendicular. From this experiment it can be concluded that under the field the director becomes oriented perpendicularly to the sample surface (dark state) and after the switching off it relaxes to a structure enforced by the planar surface anchoring. The filaments thus originate from the homeotropic state, which has been established by the field. Generally, the creation of filaments can be observed in other compounds during the SmA-TGBA phase transition for samples with the homeotropic anchoring or for the free standing films.[10-12] On cooling the filament growth slows down and below 28°C the homogeneous texture induced by the electric field persists for several tens of seconds after the field is switched off. Finally at a temperature below 27°C the dark texture persists after the field is switched off even for hours (see Fig. S1).

Unfortunately, for the temperature lower than 25°C, which corresponds to the melting point, the sample can crystallize.

The effect was observed also for ac electric field. Unfortunately, it can be observed only up to the frequency 20 Hz. For higher frequency the filaments have not enough time to expand and the texture is crumbled into tiny features. So we are losing important information about filaments orientation and growth. Additionally, the observed effect is not strictly limited to any surfactant and surface treatment. It was observed even on home-made cells without any surface treatment, see ESI and Fig. S2.

To exclude the possibility of a very narrow nematic phase above the TGBA phase, we have analyzed the mesogenic behavior of PHB(rac). The planar textures showing the phase transition from the isotropic to the SmA phase on cooling is presented in Fig. S3 (see ESI). Nuclei of the SmA phase arise in a typical form of "batonnets",[12] and immediately on further cooling a typical fan-shaped planar texture of the SmA phase appears (Fig. 5a). Under applied electric field the fan-shaped texture is irreversible changed to a perfectly aligned homeotropic SmA texture (Fig. 5b), the same effect as can be obtained for the chiral variant PHB(S) for lower temperatures (≤ 27°C). In Fig. 5a the easy direction is marked by a white arrow, the polarizers are parallel to the edge of the photo. In Fig. 5b the area under the electrodes are clearly demarked by dark homogeneous texture. Similar behavior under the applied electric field is observed in Mix 1:1, in which the Iso-SmA phase sequence is established on cooling (see ESI and Fig. S4). Contact probe was created and studied to establish the changes when mixing both racemic and chiral compounds (see ESI and Fig. S5). We have found that the concentration of both components can be continuously changed within the cell. (Fig. S5).

Table 1

Phase transition temperatures, T_c, detected on the second cooling, are in °C, the corresponding enthalpies, ΔH, are in square brackets in kJ/mol. Melting points, m.p., have been indicated on the second heating. The star means that the crystallization peak appeared on the heating thermograph in a form of the opposite peak.

	m.p./°C [ΔH/kJmol^{-1}]	T_{cr}/°C [ΔH/kJmol^{-1}]		T_c/°C [ΔH/kJmol^{-1}]
PHB(S)	25 [+25.4]	-12 [-19.5]	TGBA	33 [-3.8]
PHB(rac)	49 [+43.9]	3 [-7.2]*	SmA	35 [-4.2]
Mix 1:1	41 [+33.6]	8 [-19.2]*	SmA	33 [-3.7]

To confirm the phase identification and establish the structural parameters we performed x-ray diffraction studies on both, chiral and racemic, materials. The broad angle x-ray patterns are consistent with lamellar structure of SmA phase without any long-range molecular correlations within the layers (Fig. 6). Both studied compounds exhibit sharp Bragg reflection at low angle range reflecting layered structure of the studied mesophase and a broad diffuse maximum related to periodicity ~4.5 Å that corresponds to intermolecular distances within the layers. From the

position of the sharp low angle signal the layer spacing of smectic phase, *d*, has been determined (Fig. 7), being practically equal for both studied compounds. The temperature dependences of the layer spacing, *d*, and the signal width at half maximum, *FWHM*, are shown in Fig. 7 for both PHB(S) and PHB(rac). One can see that *d* shows the same temperature dependence and for both compounds the negative thermal expansion was observed. Concerning chiral PHB(S) exhibiting the TGBA phase below 33°C, a rather broad small-angle x-ray signal was observed even above this temperature, within 33-35°C, which is probably due to the pre-transitional effect accompanying the rise of the TGBA phase. It reflects formation of clusters with short-range SmA ordering within this temperature interval.[7] The fact that for the chiral compound PHB(S) the small-angle x-ray signal was observed above the phase transition to the TGBA phase is fully compatible with the DSC data, which show rather strong pre-transitional effect for PHB(S). In the inset of Fig. 7a the original 2D pattern is presented for PHB(S). For PHB(rac) we succeeded with better alignment, which is seen in Fig.7b as two intensive spots. In the inset of the Fig.7b the intensity was integrated over azimuthal angle Φ to yield the angular dependence, which demonstrates the orthogonal character of the molecular orientation with respect to the layer normal. The width of the x-ray signal in TGBA phase of PHB(S) has been found to be slightly higher than in the SmA phase of racemic counterpart, probably due to the worse sample alignment (compare Fig.7a and Fig. 7b). The experiments reported above have proved the existence of one smectic-like mesophase without any ordering within the smectic layers for both chiral and racemic modifications. It should be stressed that the layer spacing evaluated from the x-ray scattering data is considerable higher than the length of fully extended molecule, which was calculated to be 31 Å. Nevertheless, the similar layer spacing values for both studied compounds lead us to the conclusion, that the molecular packing of (R) and (S) molecules in smectic layers is similar to that of (S)-(S) molecules and the chirality of chains does not play principle role.

Dielectric spectroscopy studies within the frequency range 10 to 10^6 Hz have been performed for both compounds. On the planar samples not treated with the electric field, i.e. with the molecules parallel to the sample surface, the permittivity $\varepsilon_\perp$, corresponding to rotation of the molecules around their long axis, is detected. This permittivity reveals no dispersion in the frequency range studied (see Fig. 8). The observed slight increase of losses towards the low frequencies is a consequence of the ionic conductivity. Nevertheless, the ionic conductivity is very small and does not affect the observed behavior.

As mentioned above, enough strong electric field (≥10 V/μm) induces change of molecular alignment to the homeotropic orientation. In this orientation the permittivity along the long molecular axis $\varepsilon_\parallel$ is measured corresponding to the rotation of molecules about their short axis. This component exhibits a single relaxation mode with the relaxation frequency of around 10 kHz for both chiral and racemic variants. At low frequencies $\varepsilon_\parallel$ is higher than the permittivity measured on the sample without field application, where the component $\varepsilon_\perp$ prevails. The relation $\varepsilon_\parallel > \varepsilon_\perp$, known as a positive dielectric anisotropy, is the reason for the formation of the homeotropic alignment under the applied electric field. Thus, the field transformation of the

TGBA/SmA phase in the sample with the planar anchoring to the homeotropic state can be understood as an analogy of the Frederiks transition in nematics.[15]

To establish the molecular dynamics around the short axis in the whole temperature range, we used commercial cell ensuring the homeotropic geometry. We have found the relaxation process to be temperature dependent. Fitting of the measured complex permittivity dispersion of PHB(S) to Cole-Cole formula (1) yielded the temperature dependence of relaxation frequency, f_r (Fig. 9). It was found to follow the Arrhenius law, with activation energy, E_a=102 kJ/mol. This value is comparable to activation energies found for rotation of molecules around the short axis in other chiral liquid crystalline systems. [10c,12]

Discussion and conclusions

The studied PHB(S) compound exhibits the isotropic-TGBA phase sequence without any intermediate cholesteric or blue phases. In samples with planar anchoring a virgin texture of the TGBA phase exhibits typical features, namely grains with color corresponding to the length of the TGBA helical pitch, which is changing with temperature. Under an applied electric field the planar TGBA texture is reversibly transformed to the homeotropic structure, which is homogeneously dark in crossed polarizers, showing thus perfect alignment. So far such type of impact of the electric field on the TGBA phase has not been reported for any compound.

In the racemic compound PHB(rac) a monotropic SmA mesophase exists with a typical fan-shaped texture. As well as in the chiral enantiomer PHB(S), the electric field switches the planar texture to the perfectly aligned homeotropic SmA phase. In the case of PHB(rac) the switching under the electric field is irreversible and the system remains in homeotropic geometry till crystallization. The transformation of planar textures of the TGBA or SmA phases into the homeotropic SmA phase is an analogy of the Frederiks transition in nematics, in which the switching under the field is driven by the positive dielectric anisotropy. The positive dielectric anisotropy in both chiral and racemic PHB is detected up to the field frequency of about 10 kHz. So far the Frederiks transition has not been established in the TGBA phase and even in the SmA phase it is quite rare.[16] The reason might be ascertained in the complicated reversing process in smectics. While in nematics the field rotates each molecule separately, in smectics the layering prevents such a process. The reorientation of molecules would be inevitably accompanied with bending of smectic layers and a subsequent creation of numerous structural defects that cannot be expelled by the field.[17]

The transition from the planar structure to the dark homeotropic one under the field in the studied PHB compound may be easier owing to the specific packing of molecules within the smectic layers, exhibiting mutual shift of molecules within the smectic layers. Model of such layer structure is based on the structural data showing that the layer spacing is longer than the fully extended molecule. The shift of molecules might be caused by attractive forces between the benzene ring and the carbon atom from the ester bridge in the molecular core of the neighboring molecules (Fig. 10). The length of the ester linkage and of the benzene ring can get the molecular shift of about 4 Å, which fits to the estimated difference between experimental *d* value and the

molecular length. Additionally, such a model structure possesses relatively high layer compressibility, which lowers the energy of structural defects[17,18] and thus facilitates dissolving of these defects during the structure transformation. It is fully consistent with the presented effect of reorientation of molecules under the applied electric field, which has not been observed for a lamellar structure up to now.

One can point out that the positive dielectric anisotropy is the principal reason for the observed molecular reorientation under the field. Perhaps this requirement has not been fulfilled in numerous texture studies of TGBA phases known so far, where such dielectric data have not been reported. The dielectric studies have been mostly limited to the TGBC phases and/or the TGBA-TGBC phase sequences, where the collective modes occurs, connected with the formation of the spontaneous polarization.[19]

A theory describing the formation of filaments of the TGBA phase from the field induced homeotropic state is under preparation and will be published elsewhere in details. There we model and describe gradual arising of TGBA filaments from the field induced homeotropic SmA phase. Such a process is started from the sample surface and chiral forces are dominant. Finite blocks of filaments are separated from neighboring blocks of filaments by dislocation loops. The theory is able to explain the creation of filaments and their orientation with respect to the easy direction of the surface alignment. Additionally, the anchoring energy and the layer compressibility can be assessed.

The perfectly dark state of PHB compounds, induced by the electric field, either stable or reversible, might be promising for specific applications. From the application point of view, the change of the dielectric anisotropy from positive at low frequencies to negative, observed for PHB(S) at 10 kHz, might be important for high-speed photonics such as adaptive optics and diffractive optics.[20]

Acknowledgements

This work was supported by grants 13-14133S and 15-02843S (Czech Science Foundation) and project M100101211 from the Czech Academy of Sciences.

References

[1] (a) J.P.F. Lagervall and F. Giesselmann, Complexity at the nanoscale, *ChemPhysChem*, 2010, **11**, 975–977; (b) V. Novotná, M. Glogarová, V. Kozmík, J. Svoboda, V. Hamplová, M. Kašpar and D. Pociecha, Frustrated phases induced in binary mixtures of hockey-stick and chiral rod-like mesogens. *Soft Matter*, 2013, **9**, 647–653.

[2] (a) H.-S. Kitzwerow. Chirality in Liquid Crystals, Springer-Verlag, 2001, New York, 346; (b) P.P. Crooker, *Liq. Cryst*. 1989, **5**, 751.

[3] (a) L. Isaert, L. Navailles, P. Barois and H.T. Nguyen, *J. Phys. II*, 1994, 4, 1501; (b) Y. Galerne, *J. Phys. II*, 1994, **4**, 1699.

[4] (a) D. Bennemann, G. Heppke, A.M. Levelut and D. Lötzsch. Mol. Cryst. Liq. Cryst., 1995, **260**, 351; (b) M. Levelut, C. Germain, P. Keller, L. Liebert and J. Billard. *J. Phys.*

(Fr.), 1983, **44**, 623; (c) M. Levelut, E. Hallouin, D. Bennemann, G. Heppke and D. Lötzsch. *J. Phys. II*, 7, 1997, 981; (d) M. Levelut, D. Bennemann, G. Heppke and D. Lötzsch. *Mol. Cryst. Liq. Cryst*., 1997, 299, 433.

[5] P. de Genes, *Solid State Commun.*, 1972, 10, 753.

[6] S.R. Renn and T.C. Lubenski, *Phys Rev A*, 1988, 38, 2132.

[7] (a) J.W. Goodby, M.A. Waugh, S.M. Stein, E. Chin, R. Pindak and J.S. Patel. *J. Am. Chem. Soc*. 1989, 111, 8119; (b) J.W. Goodby , A.J. Slaney, C.J. Booth, I. Nishiyama, J.D. Vujk, P. Styring and K.J. Toyne, *Mol. Cryst. Liq. Cryst*., 1994, 243, 231.

[8] (a) K.J. Ihn, J.A.N. Zasadzinski, R. Pindak, A.J. Slaney and J. Goodby, *Science*, 1992, 258, 275; (b) G. Srajer, R. Pindak, M.A. Waugh and J.W. Goodby, *Phys. Rev. Lett.,* 1990, 64, 1545-1548.

[9] (a) C.W. Garland, *Liq. Cryst*., 1999, 26, 669; (b) J. Fernsler, L. Hough, R.-F. Shao, J. E. Maclennan, L. Navailles, M. Brunet, N. V. Madhusudana, O. Mondain-Monval, C. Boyer, J. Zasadzinski, J. A. Rego, D. M. Walba and N. A. Clark, *PNAS*, 2005, 102, 14191.

[10] (a) J.W. Goodby, S.J. Cowling and V. Goetz, *C.R. Chimie*, 2009, 12, 70; (b) D.S. Shankar Rao, S. Krishna Prasad, V.N. Raja, C.V. Yelamaggad and S. Anitha Nagamani, *Phys Rev Lett.*, 2001, 87, 085504; (c) N. Podoliak, V. Novotná, M. Kašpar, V. Hamplová, M. Glogarová and, D. Pociecha, *Liq. Cryst*., 2014, 41, 176.

[11] I. Dierking and S.T. Lagerwall, *Liq. Cryst.*, 1999, 26, 83.

[12] I. Dierking, *Textures of Liquid Crystals*; WILEY-CH 2003; ISBN 3-527-30725-7.

[13] M. Kašpar, V. Novotná, V. Hamplová, M. Glogarová and D. Pociecha, *Liq. Cryst.,* 2010, 37, 129.

[14] (a) M. Petit, M. Nobili and P. Barois, *European Phys. Journal B*, 1998, 6, 341; (b) M. Petit, P. Barois and H.T. Nguyen, *Europhysics Letters*, 1996, 36, 185.

[15] L.M. Blinov and V.G. Chigrinov, Electrooptic effect in liquid crystal materials. Springer-Verlag, Berlin, 1994.

[16] J. Chrusciel, J. Czerwiec, M. Jaglarz, M. Marzec, A. Wawrzyniak, M.D. Ossowska-Chrusciel and M. Wrobel, *Mol. Cryst. Liq. Cryst.*, 2011, **547**, 268.

[17] R. Holyst and P. Oswald, J. Phys. II France, 1995, **5,** 1525.

[18] M. Kleman and O. D. Lavrentovich, *Soft Matter Physics*, Chapter 10, Springer 2003, ISBN 0-387-92267-5.

[19] (a) M. Ismaili, F. Bougrioua, N. Isaert, C. Legrand, and H.T. Nguyen, *Phys. Rev.,* 2001, 65, 011701; (b) M.R. Dodge, J.K. Vij, S.J. Cowling, A.W. Hall, and J.W Goodby, *Liq. Cryst*., 2005, 32, 1045; (c) A.S. Pandey, R. Dhar, M.B. Pandey, A.S. Achalkumar, and C.V. Yelamaggad, *Liq. Cryst.*, 2009, 36, 13.

[20] H. Xianyu, S.-T Wu and C.-L. Lin, *Liq. Cryst*., 2009, 36, 717.

Figure Captions:

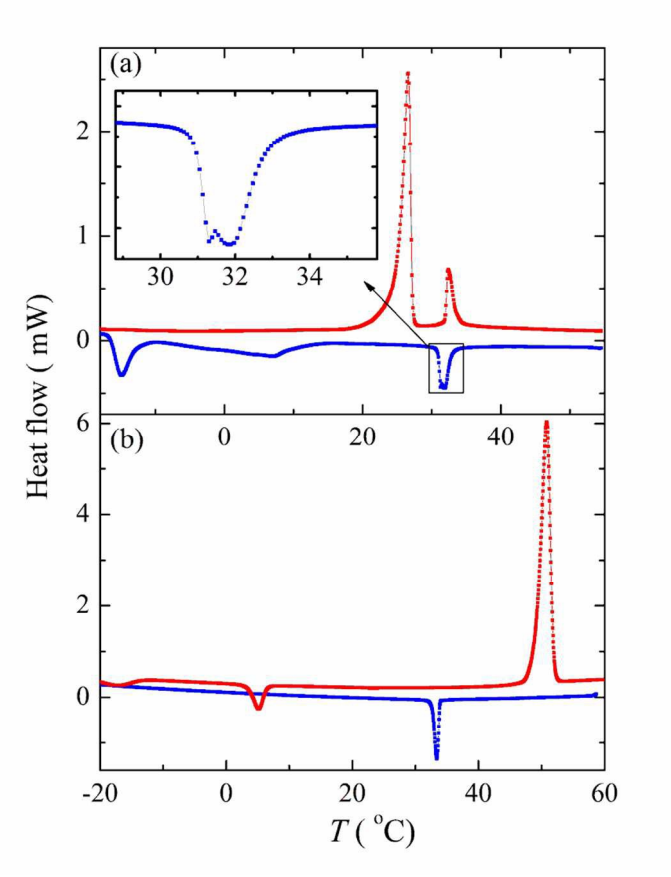

Fig.1
DSC plots for (a) chiral PHB(S) and (b) PHB(rac), taken on the second heating (upper) and the subsequent cooling (lower curve) at a rate of 5 K min^{-1}. The upper curves (red) show the second heating and lower curves (blue) the second cooling runs.

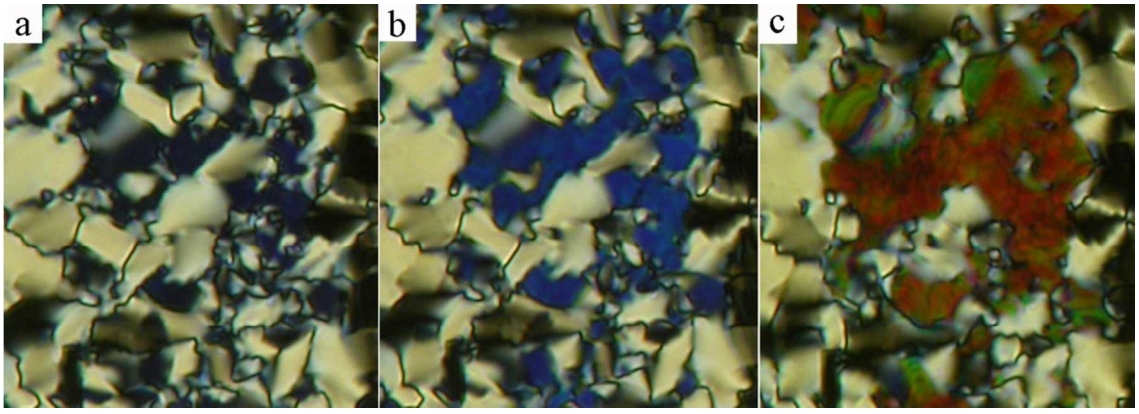

Fig. 2
Planar textures for PHB(S) in dependence of temperature: (a) T=32.8°C, (b) T=32.4°C, and (c) T=31.9°C. The width of every photo corresponds to about 150 μm.

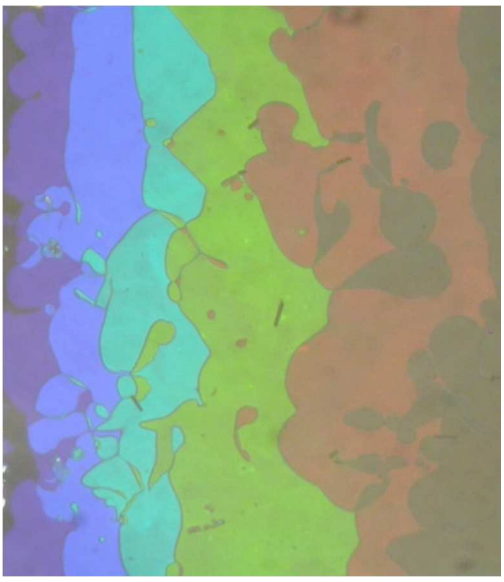

Fig. 3
Planar texture in temperature gradient, the temperature at the left side T= 32.9°C and the right side T= 31.8°C for PHB(S). The width of the photo corresponds to about 250 μm.

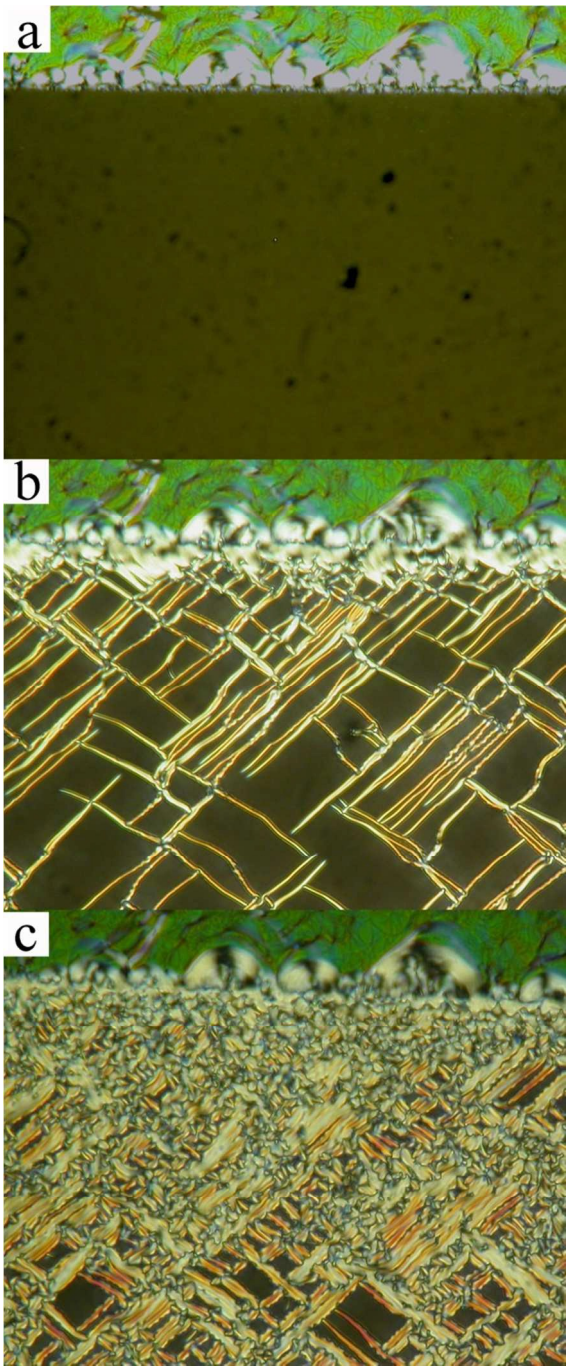

Fig. 4
For PHB(S) the evolution of the filament texture after the electric field treatment at a temperature T=30°C. In the upper part of the sample there is the original virgin planar texture. The horizontal boundary is the upper edge of the electrode, which is parallel to the easy direction. (a) homeotropic orientation under the electric field, (b) nucleation of filaments after the field switching off, (c) the filaments flow together and the texture gradually changes. The width of the photo corresponds to about 250 μm.

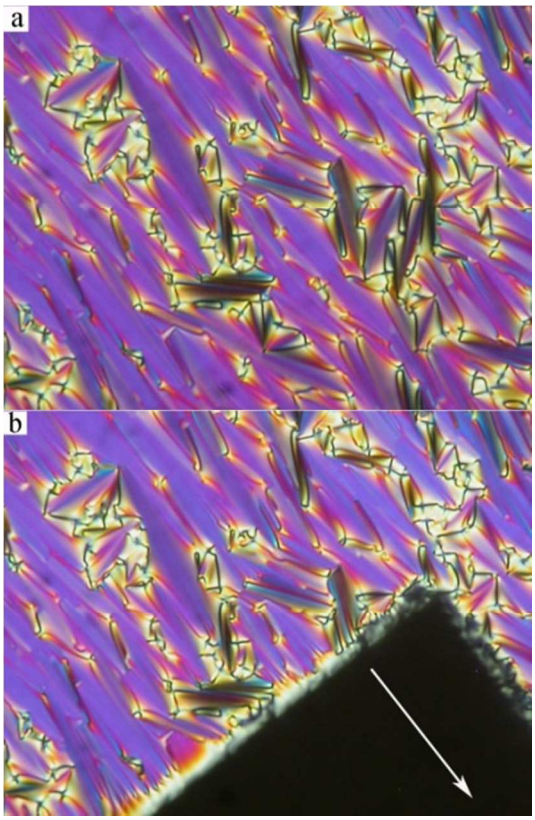

Fig. 5
The SmA planar texture in the PHB(rac): (a) no field applied, (b) after the field application the planar texture below the electrode remains dark. The easy direction is marked by a white arrow and the polarizers are parallel to the edge of the photo. The width of the photo corresponds to about 300 μm.

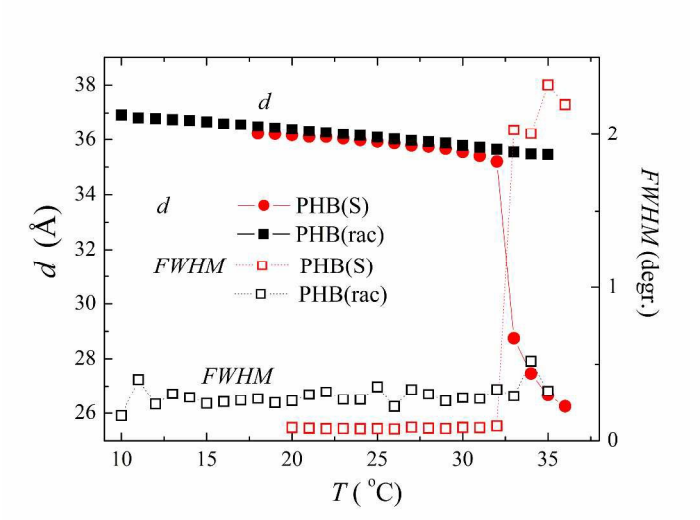

Fig. 6
Layer spacing, *d*, determined from the position of a low angle x-ray signal and the signal width at half maximum, *FWHM*, for both PHB(S) and PHB(rac).

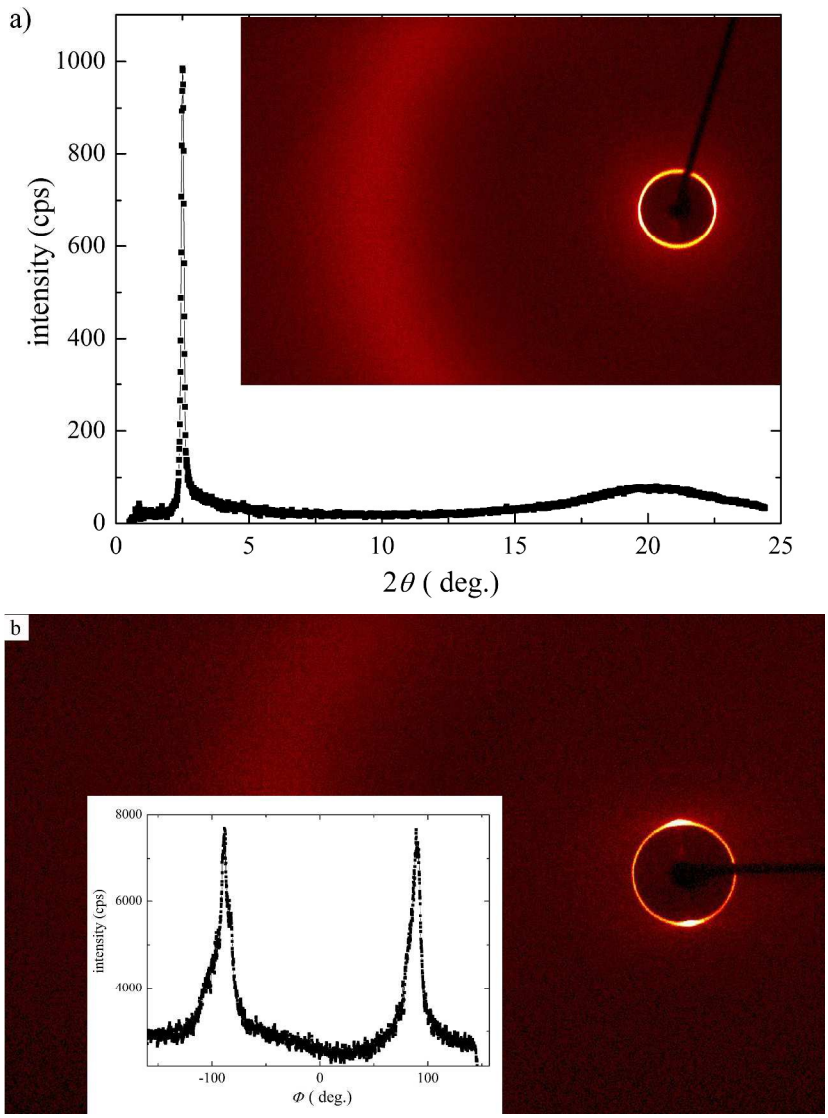

Fig. 7

(a) X-ray intensity in dependence on diffracted angle, θ, for PHB(S). In the inset 2D x-ray pattern is presented. (b) For PHB(rac) the original 2D pattern is shown and in the inset the corresponding intensity was integrated over azimuthal angle Φ to yield the angular intensity dependence. Both x-ray measurements were performed at the temperature T=26°C

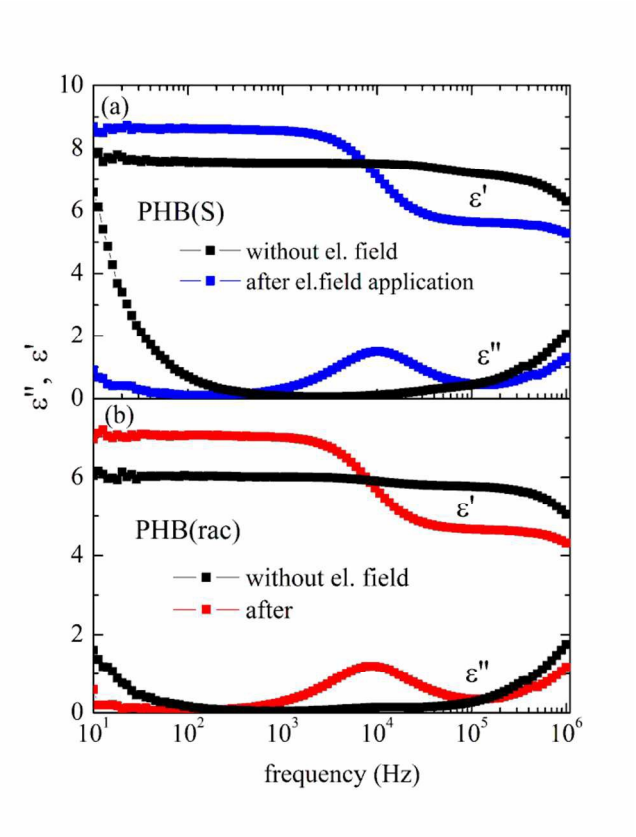

Fig. 8
Real, ε', and imaginary, ε'', parts of permittivity, measured before and after the field application for PHB(S) and PHB(rac) at a temperature T=28°C.

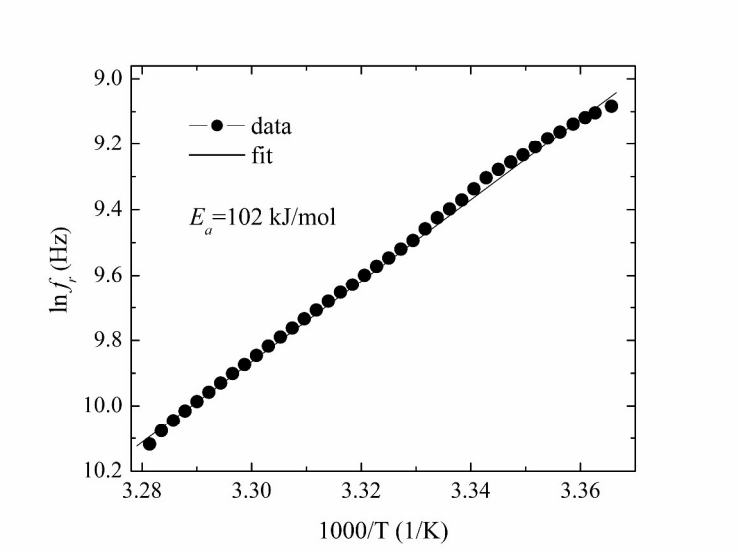

Fig. 9
Arrhenius law showing the relaxation frequency, f_r, in a logarithmic scale versus the inverse temperature in Kelvins, 1/T. f_r, values were obtained by fitting of the dielectric spectroscopy data using (1) formula.

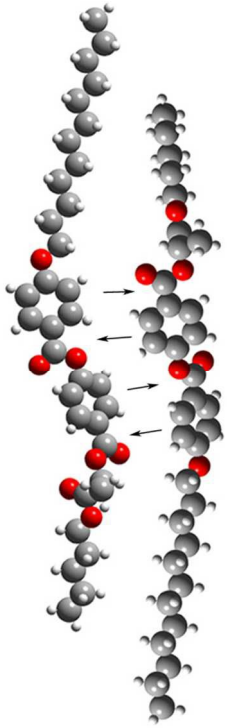

Fig. 10
Model of packing of molecules in the smectic layer. Arrows show attractive forces between benzene rings and carbon from the ester bridge.

	m.p./°C [ΔH/kJmol^{-1}]	T_{cr}/°C [ΔH/kJmol^{-1}]		T_c/°C [ΔH/kJmol^{-1}]
PHB(S)	25 [+25.4]	-12 [-19.5]	TGBA	33 [-3.8]
PHB(rac)	49 [+43.9]	3 [-7.2]*	SmA	35 [-4.2]
Mix 1:1	41 [+33.6]	8 [-19.2]*	SmA	33 [-3.7]

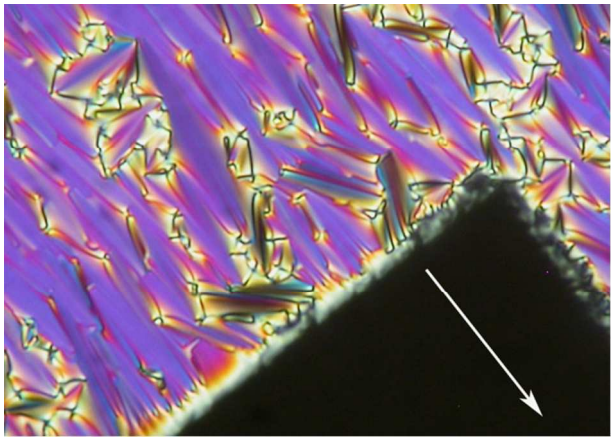

Unique effect is observed in TGBA phase under applied electric field, which reversibly transforms the planar texture to homeotropic one.